Soft Matter

Cite this: *Soft Matter*, 2011, **7**, 6719

www.rsc.org/softmatter

PAPER

Bouncing bubble on a liquid/gas interface resting or vibrating

Jan Zawala,*[a] Stéphane Dorbolo,[b] Denis Terwagne,[b] Nicolas Vandewalle[b] and Kazimierz Malysa[a]

Received 2nd March 2011, Accepted 4th May 2011
DOI: 10.1039/c1sm05365e

The bouncing of air bubbles of about 1 mm in diameter on an air/oil interface is reported. We compare the behavior of the bubble when the interface is at rest or when it is vibrated. The results obtained for the interface at rest allowed extracting the key parameter responsible for the outcome of the bubble collision, *i.e.* bounce or coalescence (bubble rupture). This parameter is the deformation of the bubble. When the bubble deformation is sufficient (according to the oil viscosity and to the bubble velocity and size), the bubble bounces because the intervening oil film has a large radius and the bubble–interface contact time is much shorter than the time needed for the film drainage to its critical thickness of rupture. This hypothesis is confirmed by the experiments of the bubble collisions with vertically vibrated air/oil interface. It was shown that it is possible to significantly increase the bubble lifetime: the bubble bounces at the interface when the interface is vibrated, and this occurs when the vibration amplitude is above a threshold. The amplitude threshold depends on the frequency, on the size of the bubble and on the viscosity of the surrounding oil. For bouncing, the vibrated interface must provide enough energy to the bubble to deform in such a way that the drainage characteristic time of the oil film becomes longer than the contact time between the bubble and the interface.

Introduction

Bubble formation, motion and especially collisions with an interface are highly dynamic processes and their outcome depends not only on the properties of the interface but also on the motion of the bubble. For example, even in the case of distilled water the colliding bubble can bounce a few times at a free surface. The rebound of an air bubble at free liquid interface has been carefully studied theoretically and experimentally in water[1–7] and in other liquids.[8,9] In the majority of cases the experiments were carried out in pure liquids, devoid of any surface-active substances, *i.e.* in the simplest possible systems for investigation of the mechanism of the bubble bouncing and coalescence.

The experimental investigations reported in the literature aimed at the determination of the so-called coalescence time (t_c), defined as the time elapsed between the moment of contact with the interface and the rupture of the liquid film formed.[1] The t_c values are highly affected by the number of bounces before its rupture at the liquid/air interface[6–9] and by the velocity of the bubble approaching the interface.[1,3–5,7–9] Actually, it was observed that t_c increases significantly with the bubble impact velocity, because high velocity prolonged the bubble bouncing. Moreover, the amplitude of the bubble bouncing decreases in each subsequent collision. This indicates that the kinetic energy is dissipated after the successive shocks.[10] The velocity of the bubble is a very important factor that affects the outcome of the bubble collision. However, no suitable and full explanation of the mechanism of the bubble bouncing and rupture was given.

The properties of the interface are a common feature of bubbles and droplets moving in pure, devoid of surfactants, liquids. Since the seminal Couder's[11] in 2005, the bouncing of a droplet on a liquid bath has provided very fine work with surprising results in several fields including even quantum mechanics.[12,13] The summary of these investigations is that a droplet can bounce on a liquid bath when this bath is vertically and sinusoidally shaken above a critical value of the amplitude, A, that depends on the considered frequency, f, the surface tensions of both phases (σ_1, σ_2), the viscosities of the liquids composing the droplet (η_1), the bath (η_2), the size of the droplet and the viscosity of air. Above this critical acceleration $\Gamma_c = A(2\pi f)^2/g$, the intervening air film squeezed between the droplet and the bath can be renewed at each bounce. That mechanism prevents the droplet from coalescing. For large droplets (diameter about 1 mm), droplet deformations have been shown to be the governing process that allows to explain the existence of possible minima in the critical amplitude values with respect to the frequency.[14,15] Indeed, a resonance phenomenon occurs in the system droplet–intervening air film. This process allows permanent bouncing for acceleration even below the gravity. Is it possible to make an air bubble bouncing practically indefinitely

[a]*Jerzy Haber Institute of Catalysis and Surface Chemistry Polish Academy of Sciences, ul. Niezapominajek 8, 30-239 Krakow, Poland. E-mail: ikifp@cyf-kr.edu.pl; Fax: +48 12 4251923; Tel: +48 12 6395101; nczawala@cyf-kr.edu.pl*
[b]*GRASP, Physics Department B5, University of Liège, Allée du VI août, 17, B-4000 Liège, Belgium. E-mail: s.dorbolo@ulg.ac.be; Fax: +3243663607; Tel: +3243663656*

at the liquid/air interface? This question is the central focus of the present article.

In this paper, we investigate the possibility of bouncing of an air bubble at the interface between air and silicone oils. The influence of three parameters influencing the t_c has been studied: (i) bubble size and impact velocity, (ii) amplitude (A) and frequency of the applied vibrations, (iii) viscosity of the oil. This work is partitioned into two main kinds of experiments. The first kind concerns the behaviors of the air bubble rebounding at the air/oil interface when the latter is at rest. This case serves as a reference to the second kind of experiments when the air/oil interface is shaken.

Experimental

Observations of a single bubble collision with the liquid/air interface were performed with a set-up that consisted of: (i) a square glass column (45 × 45mm) with the capillary tube at the bottom, (ii) a precise system of the gas dosage (syringe pump), (iii) high speed camera (1000 Hz, 1024 × 1024 pix), and (iv) an electromagnetic shaker connected to oscilloscope and amplifier. Fig. 1 presents schematically the experimental set-up. Capillaries with inner diameters 0.025, 0.050, 0.10 and 0.17 mm were used in the experiments. The bubble was formed at the capillary orifice and, after detachment, its motion and collisions with the liquid/gas interface, located at a distance of *ca.* 7 cm above the capillary, was monitored and recorded using a high speed camera. To calibrate the measurements, the image of a nylon sphere of 5.89 mm diameter was recorded after each experiment to convert the pixel size into millimetres. The movies recorded were saved on the hard disk and the bubble dimensions and velocities were determined on the basis of image analysis using the SigmaScan Pro Image Analyze Software and/or the WinAnalyze Motion Analyze Software. Variations of the bubble velocity were determined from measurements of the positions of the bubble bottom pole on the successive frames of the movie.

The observations and monitoring of the phenomena occurring during the bubble collisions with the liquid/air interface were carried out for: (i) the interface being at rest, and (ii) the interface vibrating, with controlled frequency and amplitude. Square Plexiglas cap (40 × 40mm) was fixed to the shaker moving table.

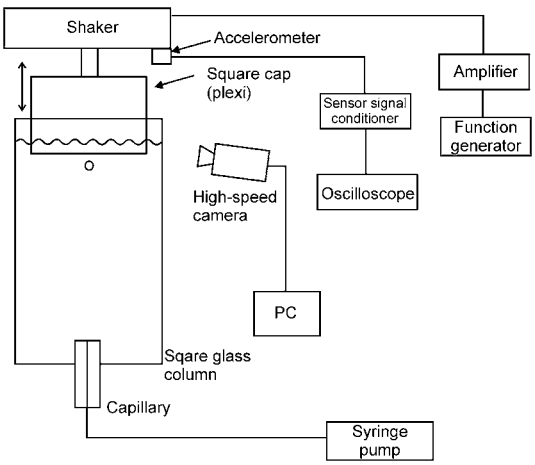

Fig. 1 Experimental set-up.

The cap was gently inserted (*ca.* 10 mm) into the liquid in such a way as to avoid contact with the walls of the square glass column. The camera was slightly tilted (angle of inclination 3–4°) to observe the phenomena occurring beneath the vibrating liquid surface during bubble collision and bouncing. In order to control the acceleration of the vibrations applied, an accelerometer was connected to the shaker plate.

The square glass column was filled with DOW CORNING 200® FLUID silicone oil of two different viscosities - $\nu = 0.65 \times 10^{-6}$ and 1.5×10^{-6} m^2 s^{-1}, chosen for the experiments. The details of the liquid used are presented in Table 1.

Results and discussion

To determine the size and shape deformation of the bubbles the horizontal (d_h) and vertical (d_v) diameters of the bubbles were measured during its approach and collision with the oil surface. For the stage of bubble approach to the interface (before collision) the bubble equivalent radius (R_b) was determined as $R_b = 0.5(d_v d_h^2)^{1/3}$. Additionally the theoretical bubble radius (R_{eq}^{th}) was calculated, according to Tate's law,[16,17] resulting from the interrelation between the buoyancy and capillary forces. Table 2 presents the results and there is generally a good agreement between the R_b and R_{eq}^{th} values. Some differences between experimentally determined and theoretically calculated bubble diameters can be noted only for the capillary of the largest inner diameter (0.17 mm). Additionally, the values of the bubble terminal velocities (U_t) are given in Table 2. The range of the Reynolds number ($Re = 2R_bU_t/\nu$) for the bubbles rising in the liquids studied was 380–540 and 110–205 for lower and higher oil viscosity, respectively.

Surface at rest: effect of the bubble size and liquid viscosity

A sequence of the snapshots illustrating the bubble collision (R_b = 0.40, 0.53 and 0.54 mm) with free oil surface (viscosity 0.65×10^{-6} and 1.5×10^{-6} m^2 s^{-1}) being at rest are presented in Fig. 2. As can be observed, the shape of the larger bubbles (R_b = 0.53 and

Table 1 Properties of the silicone oils used in the experiments

No.	Viscosity,ν/m^2 s^{-1}	Specific gravity	Density, ρ/kg m^{-3}	Surface tension, σ/mN m^{-1}
1.	0.65×10^{-6}	0.750	750	15.9
2.	1.5×10^{-6}	0.850	850	16.8

Table 2 Terminal velocities and theoretically calculated and experimentally determined sizes of the bubbles

		Kinematic viscosity/m^2 s^{-1}					
		0.65×10^{-6}			1.5×10^{-6}		
No.	Capillary inner diameter/mm	U_t/cm s^{-1}	R_b/ mm	R_{eq}^{th}/ mm	U_t [cm s^{-1}]	R_b [mm]	R_{eq}^{th} [mm]
1.	0.025	16.8 ± 0.5	0.32	0.34	10.6 ± 0.7	0.33	0.34
2.	0.050	22.3 ± 0.4	0.43	0.43	15.0 ± 0.7	0.40	0.42
3.	0.10	23.6 ± 0.5	0.54	0.55	18.2 ± 0.5	0.53	0.53
4.	0.17	24.0 ± 0.5	0.56	0.65	19.6 ± 0.3	0.58	0.64

0.54 mm) was significantly more deformed at the approach stage of the motion and during its collisions with the oil surface and bouncing. Moreover this effect was significantly larger in oil of lower viscosity ($\nu = 0.65 \times 10^{-6}$ m^2 s^{-1}—see insert in Fig. 2). Additionally, the lifetime of larger bubbles was longer at the oil/air interface because the bubble of larger radius bounced a greater number of times before rupture. As illustrated in Fig. 2 the bubble of $R_b = 0.53$ and 0.54 mm collided with the interface three and four times, respectively, prior to the rupture, while the bubble of $R_b =$ 0.40 mm only twice. Note also that the bubble shape deformations decreased with collision number, due to dissipation of the kinetic energy associated with the bubble motion.

The results of analysis of the velocity during collisions of bubbles of different sizes with oil/air interface are presented in Fig. 3 for oils of viscosity 0.65×10^{-6} m^2 s^{-1} (Fig. 3A) and 1.5×10^{-6} m^2 s^{-1} (Fig. 3B). Negative velocity values mean that the bubble had bounced and moved downward. The moment of the bubble's first collision with the interface was arbitrary chosen as the time $t = 0$. Negative time values refer to approach stages of the rising bubbles. As can be observed, the bubbles approached the interface with constant velocity, *i.e.* terminal velocity U_t. The colliding bubbles were rapidly slowed down, stopped (velocity = 0 cm s^{-1}) and bounced in a very short time (*ca.* 5 ms). Then, the bubbles started their second approach to the interface. The time corresponding to the bubbles' rupture is marked in Fig. 3. It is clearly seen that the time of the bubbles' rupture, t_c, depends on the bubble size, liquid viscosity and is related to the number of rebounds. The t_c values increase with the bubble radius and in the case of oil viscosity 0.65×10^{-6} m^2 s^{-1} they are equal to 12, 32, 51 and 53 ms for R_b 0.32, 0.43, 0.54 and 0.56 mm, respectively. In oil of higher viscosity (1.5×10^{-6} m^2 s^{-1}) the t_c values were 7, 11, 26 and 32 ms for the bubbles of radius R_b = 0.33, 0.40, 0.53 and 0.58 mm, respectively. Note also that velocities of the first collision were smaller in oil of higher viscosity. It needs to be underlined here that the bubble collisions and bouncing are very fast processes and therefore each experiment was repeated 20 times to check reproducibility. Fig. 4 presents the statistics of this reproducibility check. The bouncing statistics are represented for the bubbles of four different sizes colliding with a free surface of oils of viscosity 0.65×10^{-6} and 1.5×10^{-6} m^2 s^{-1}. The results obtained are presented as a probability of rupture *versus* the collision number, *i.e.* the numbers of collisions needed for the bubble to pop according to their size. The sizes of the bubbles are expressed in Fig. 4 in term of the inner diameters of the capillaries used for the bubbles' formation because the sizes of the bubbles, formed in different oils at the same capillary, can be a bit different (see Table 2). As can be observed in Fig. 4 the reproducibility of the bouncing was excellent for all bubble sizes in the case of the oil with viscosity 1.5×10^{-6} m^2 s^{-1}. In the case of oil with viscosity 0.65×10^{-6} m^2 s^{-1}, reproducibility of 100% was observed only for the smallest bubbles. In the case of larger bubbles, the distribution of the number of collisions before the rupture has a wider spread. Note also that the bubble's tendency to bounce was larger in oil with smaller viscosity, for which the bubble's approach velocity was higher and the shape deformation was larger (see Fig. 2 and 3). Let us discuss the possible reasons for the differences in the bubble bouncing and the lifetime at the free surface of oils with different viscosity.

Fig. 5 presents the snapshots of the bubbles with a practically identical size (R_b = 0.54 and 0.53 mm for 0.65×10^{-6} and 1.5×10^{-6} m^2 s^{-1}, respectively) just before and during the 1st and subsequent collisions with the surface of oils with viscosities 0.65×10^{-6} and 1.5×10^{-6} m^2 s^{-1}. The pictures showing the bubbles are presented in parallel when the deformation is maximal during the considered collision. The photos of Fig. 5 clearly illustrate that the bubble was more deformed in oil with 0.65×10^{-6} m^2 s^{-1} and that the degree of deformation decreases with the collision number since the impact velocity decreases (see also Fig. 3). Fig. 6 presents the quantitative data for all bubble sizes studied on their maximum deformation during the collisions with the oil free surface. These deformation variations are defined as the maximum of the horizontal diameters during the bubble successive collisions with free surface of oils with viscosities 0.65×10^{-6} and 1.5×10^{-6} m^2 s^{-1}. As can be observed, the bubble shape deformations were larger in the oil of smaller viscosity and, as a rule, the deformations decrease with the collision number, *i.e.* with the bubble impact velocity.

The bubble rupture occurs when the oil film separating the colliding bubble from the air phase breaks. As was shown elsewhere[10] the dynamic radius (R_F) of the liquid film formed depends on the horizontal diameter (d_h) of the colliding bubble and can be estimated using the following relation:

$$(R_F)^2 = \frac{E_k d_h}{2\pi\sigma_{eq}\Delta d_v} \quad (1)$$

where σ_{eq} is the liquid surface tension, Δd_v is a change in vertical diameter of the bubble just before collision, $E_k = f(F_{dyn})$ is the kinetic energy associated with the bubble motion, and F_{dyn} is a temporary force.[10] The physical meaning of this temporary force (F_{dyn}), squeezing out liquid from the intervening film, is that it is the force executing the work of the bubble shape deformations, carried out at the distance of the bubble deformation during the collision. Thus, the larger E_k and d_h values mean that the radius of the film formed by the colliding bubble is increased. The larger size of the thin liquid film formed means that longer time is needed for the film drainage to reach its critical thickness of rupture. The third collision of the bubble in oils with viscosities 0.65×10^{-6} and 1.5×10^{-6} m^2 s^{-1} (see Fig. 5) is a good example of understanding this mechanism. The third collision of the bubble for $\nu = 1.5 \times 10^{-6}$ m^2 s^{-1} corresponded to the rupture of the film, *i.e.* the collision during which the separating liquid film reached its critical thickness. In the case of $\nu = 0.65 \times 10^{-6}$ m^2 s^{-1} oil the bubble bounced during the third collision, *i.e.* the liquid film did not reach its rupture thickness despite the liquid being less viscous. Comparing the deformation of the bubble during the 3rd collision for oils with $\nu = 0.65 \times 10^{-6}$ and 1.5×10^{-6} m^2 s^{-1} one can observe that the bubble shape deformation was larger for less viscous oil. This effect is clearly seen in the data presented in Fig. 6. There are variations of the bubble horizontal diameter presented at collision, called d_h maximum, with the collision number. When the rupture occurred, the horizontal diameters for a definite bubble initial size were quite similar in both oils, which indicates that the liquid film plays the decisive role.

In the case of one component liquids, devoid of any surfactant, the velocity of liquid film thinning (film drainage velocity) is determined mainly by the force causing the drainage, radial dimensions of the draining film and the viscosity of the liquid.

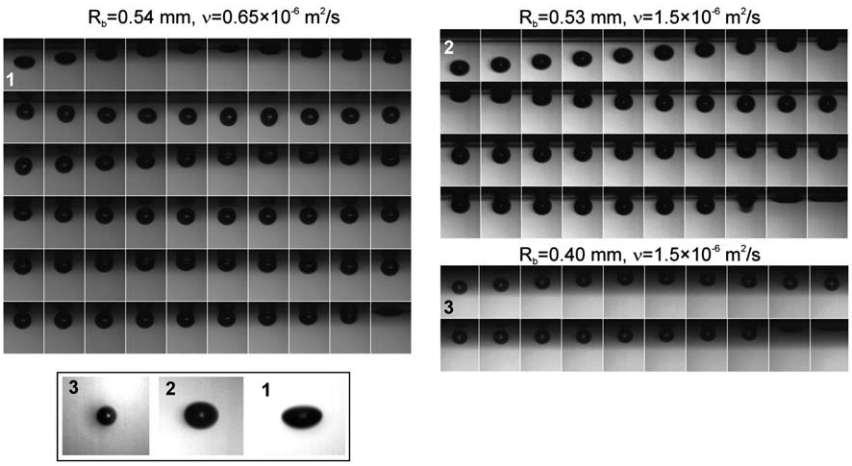

Fig. 2 Sequences of photos illustrating bouncing and coalescence of the bubbles with radius $R_b = 0.54$, 0.53 and 0.40 mm with the resting surface of oils with viscosity $\nu = 0.65 \times 10^{-6}$ and 1.5×10^{-6} m^2 s^{-1}. Time interval between the subsequent photos, $\Delta t = 1$ ms. Inserts show shape deformation of the bubble of radius $R_b = 0.53$mm at the approach stage to the oil/air interface.

Generally, the time of the film drainage to reach a given thickness increases with the film size. Unfortunately, all models of the liquid films thinning refer to the creeping flow conditions (Re < 0.01) and, as far as we know, there is lack of any model for flows at high Reynolds numbers. Therefore, the Scheludko equation[18] valid for the creeping flow conditions was used as an approximation to estimate the importance of the film size in the drainage kinetics. According to the Scheludko equation[18] the kinetics of the liquid film drainage is given as:

$$\frac{d(1/h^2)}{dt} = \frac{4}{3} n \frac{\Delta p}{\nu \rho R_F^2} \quad (2)$$

where n is the factor for mobility of the film interfaces, ν is kinematic liquid phase viscosity, Δp (capillary pressure) is the driving force of the film thinning, h is the film thickness and t is the film drainage time. After integration and rearrangement, eqn (2) can be rewritten as:

$$t = \frac{3}{4n} \cdot \frac{\nu \rho R_F^2}{\Delta p} \cdot \left(\frac{1}{h^2} - \frac{1}{h_0^2} \right) \quad (3)$$

where h_0 is the initial film thickness. Eqn (3) shows that the drainage time is directly proportional to the liquid viscosity, the radius of the film formed (in second power!) and inversely proportional to the driving force (Δp) causing the film thinning. Under dynamic conditions the driving force (Δp) causing the film drainage is related to the kinetic energy (E_k) associated with the bubble motion[10] and is given by:

$$F_{dyn} = \frac{E_k}{\Delta d_v} \quad (4)$$

where Δd_v is a change in vertical diameter of the bubble just before collision, and that, at the moment of the bubble's maximum deformation, the driving force (ΔP) can be expressed[10] as:

$$\Delta P = \frac{F_{dyn}}{\pi R_F^2} \quad (5)$$

We obtain, after substituting the relations (4) and (5) into eqn (3), that:

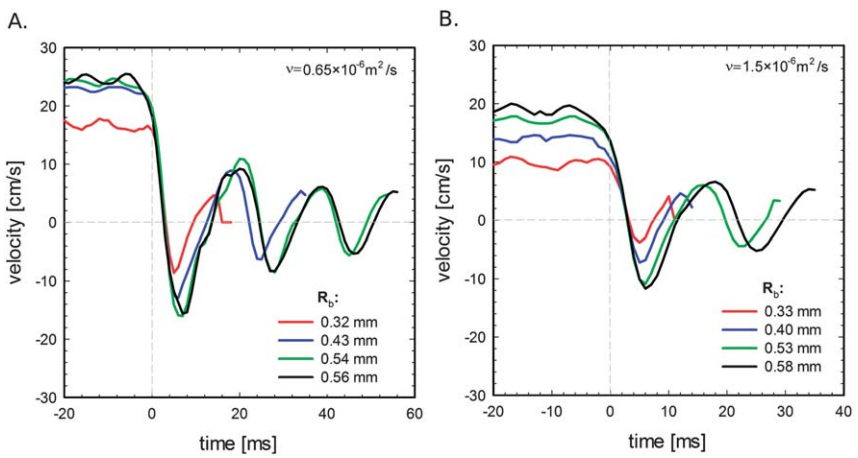

Fig. 3 Velocity variations of the bubbles with different sizes bouncing from free surface of oils with viscosity (A) 0.65×10^{-6} m^2 s^{-1} and (B) 1.5×10^{-6} m^2 s^{-1}.

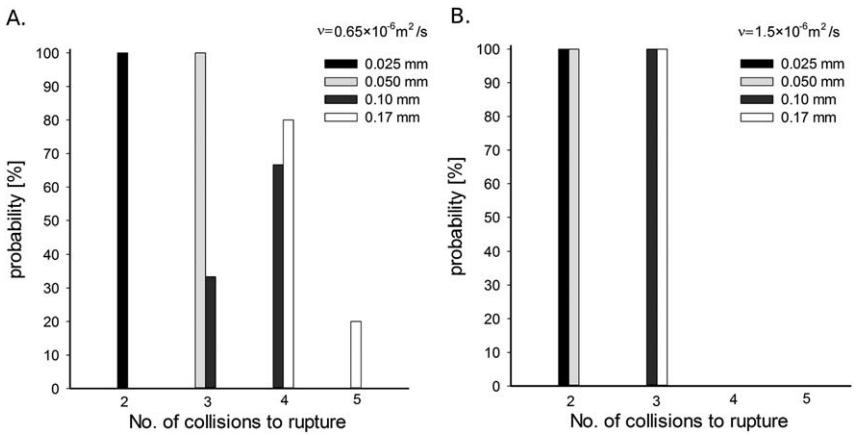

Fig. 4 Percentage of the bubbles, formed at capillaries with inner diameters 0.025, 0.050, 0.10 and 0.17 mm, rupturing during the 2nd, 3rd, 4th and 5th collision with a free surface of oils with viscosity $\nu = 0.65 \times 10^{-6}$ and 1.5×10^{-6} m^2 s^{-1}.

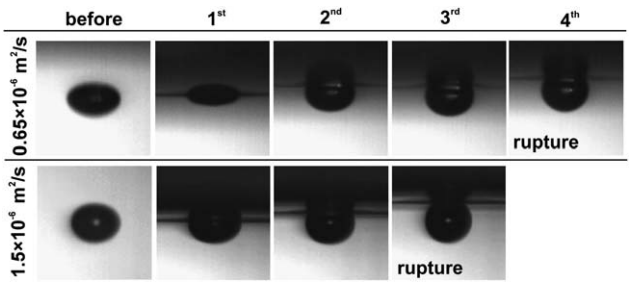

Fig. 5 Shapes of the bubble just before and during the collisions with a free surface of the oils with viscosities $\nu = 0.65 \times 10^{-6}$ and 1.5×10^{-6} m^2 s^{-1}.

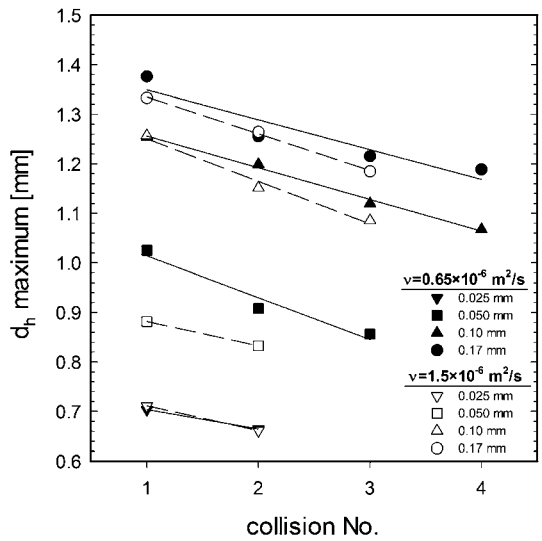

Fig. 6 Maximum values of the bubble horizontal diameter at collisions with a free surface of oils with viscosities $\nu = 0.65 \times 10^{-6}$ and 1.5×10^{-6} m^2 s^{-1}.

$$t = \frac{3}{4n} \cdot \frac{\pi \nu \rho R_F^4 \Delta d_v}{E_k} \cdot \left(\frac{1}{h^2} - \frac{1}{h_0^2} \right) \quad (6)$$

Eqn (6) clearly demonstrates the dominating effect of the size of the liquid film formed. Indeed, the time for the film to be drained out to the thickness of rupture varies with the fourth power of the film radius. Thus, the size of the liquid film formed by the colliding bubble is the parameter of the highest importance for the kinetics of the film drainage.

It was showed elsewhere, for bubble collisions with the water/air interface[10] and demonstrated above (Fig. 4) that the coalescence time at the liquid/air interface depends on the bubble impact velocity. When the bubble impact velocity decreases the coalescence time shortens. As described above, the amplitude of the bubble bouncing and the impact velocity of each subsequent collision decrease due to dissipation of the kinetic energy associated with the bubble motion. Thus, if there would be no energy dissipation or the dissipated energy would be supplied from an external source, then the bubble bouncing should be prolonged and deformations of the bubble shape should not change with the collision number. If it takes place it would be a strong evidence confirming the crucial role of the film size in the bouncing mechanism. The results of the experiments with the vibrating free surface, reported below, show that it is the case.

Effect of liquid surface vibrations

In the case of the air/oil interface being at rest, the amplitude of the bouncing and the bubble shape deformation are smaller and smaller in each subsequent collision due to dissipation of the kinetic energy associated with the bubble motion. The energy dissipated during the collision can be added (re-supplied) from an external source, for example by vibrating the oil/liquid interface with a proper frequency (f) and amplitude (A). If this energy restitution is properly compensated by the vibrating interface, the bubble impact velocity at each subsequent collision should stay constant. Consequently, the bubble shape deformation and the size of the liquid film formed should also be constant and the bubble should continue its bouncing without rupture.

Fig. 7 presents a comparison of the bubble velocity variations during its collision with the surface at rest (see also Fig. 3) and the vibrating surface. As seen, the velocity of the bubble colliding with the oil free surface at rest systematically

decreases in each subsequent collision and the bubble ruptured during the fourth collision. In the case of the vibrating surface the story is completely different. The bubble impact velocity was similar at each successive collision with the vibrating oil/gas interface. Consequently, the bouncing can be prolonged almost indefinitely. It shows that due to surface waves generated at the free surface the kinetic energy dissipated during the collisions was restituted and the impact velocity was kept constant.

Fig. 8 compares snapshots of a bubble during its subsequent collisions with the vibrating interface and of a bubble colliding with the oil/air interface at rest (1.5×10^{-6} m^2 s^{-1}). The maximum deformation of the bubble shape does not qualitatively change during collisions with the vibrating interface, while for the oil interface at rest, the bubble deformation diminishes with the collision number. Fig. 9 presents quantitative data on the shape deformation of the bubbles in oils with viscosities 1.5×10^{-6} m^2 s^{-1} (Fig. 9A) and 0.65×10^{-6} (Fig. 9B). Fig. 9A presents the bubble horizontal diameter at collision as a function of the collision number in oil with $\nu = 1.5 \times 10^{-6}$ m^2 s^{-1}. That figure shows that whatever the diameter, the deformation remains constant with the number of bounces when the bath is vibrated. The constant value depends on the bubble size. Fig. 9 presents a comparison of variations of the bubble deformation with $R_b = 0.56$ mm during its collision with the $\nu = 0.65 \times 10^{-6}$ m^2 s^{-1} oil surface at rest and vibrating. Quite an opposite effect is observed at the oil/air interface being at rest, where the bubble horizontal diameter decreases rapidly with the collision number (Fig. 9B).

When the surface is at rest, the impact velocity of the bubble decreases due to energy dissipation. As a result, during the fourth collision the bubble deformation and the radius of the liquid film formed became so small that it was possible for the film to drain to its rupture thickness. For the vibrating surface, due to additional energy supplied by the surface waves, the radius of the liquid film formed was constant and too large to reach its critical thickness of the rupture during the collision time. Thus, the "preservation" of a larger film size was the reason of prolongation of bubble bouncing and the coalescence

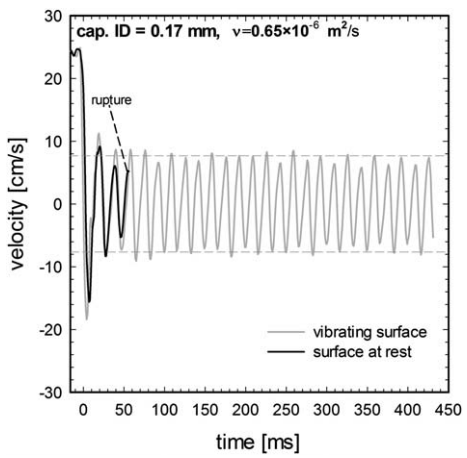

Fig. 7 Variations of the bubble velocity during its bouncing at the oil/air interface being at rest and vibrating ($f = 61$ Hz, $A = 160$ mV).

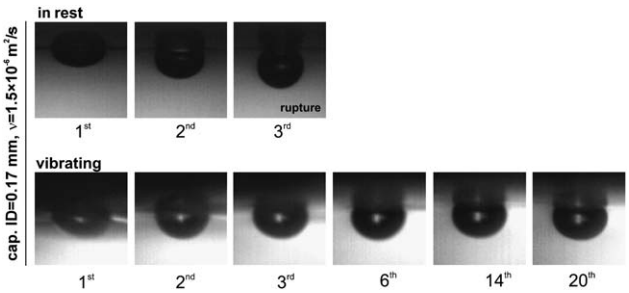

Fig. 8 Comparison of the bubble shape during subsequent collisions with a resting (top row) and vibrating (bottom row) oil/air interface. The bubbles were formed at 0.17 mm capillary orifice in oil with viscosity 1.5×10^{-6} m^2 s^{-1}.

time at a vibrating liquid surface. This bouncing bubble is similar to a ball bouncing on a vibrated plate. In the bouncing ball problem, the ball bounces once per period and locks at a constant phase that is a function of the coefficient of restitution.[19] In the bubble case, the coefficient of restitution role is played by deformation and thus depends on the impact velocity.

Let us estimate the radius of the liquid film formed during the bubble collision with the oil/air interface using eqn (1). Fig. 10 presents a comparison of the estimated dynamic radius of the film formed by the bubbles with radius $R_b = 0.56$ mm and $R_b = 0.40$ mm colliding with the surface vibrating and being at rest for oils with viscosities $\nu = 0.65 \times 10^{-6}$ m^2 s^{-1} and 1.5×10^{-6} m^2 s^{-1}. In the case of the surface at rest the R_F values refer to the film formed during collision of the bubble rupture. For a vibrating surface the R_F values presented were calculated as an average from 15 collisions. As can be seen, the size of the film formed at a vibrating surface is much larger in comparison with the surface at rest. In the case of the surface at rest the size of the liquid film at the moment of its rupture for oil with $\nu = 0.65 \times 10^{-6}$ m^2 s^{-1} is equal to 0.20 mm, while for $\nu = 1.5 \times 10^{-6}$ m^2 s^{-1} the value is 0.14 mm. The average radii of the film formed during the bubble collisions with the vibrating surface were 0.31 and 0.23 mm, respectively, *i.e.* significantly larger. These results show clearly the crucial role of the liquid film radius for the mechanism of the bubble bouncing at the oil/air interface and are in accordance (a good correlation) with data on the mechanism of the bubble bouncing at the water/air interface.[10] When the size of the liquid film formed is kept practically constant at the vibrating interface, due to additional energy supplied by the surface waves, then the bubble continues bouncing and coalescence does not occur.

Additional experimental findings show that the frequency and amplitude of the oil/air interface vibrations must be tuned for each bubble size studied. For example, in the case of vibrating oil/air interface with $\nu = 1.5 \times 10^{-6}$ m^2 s^{-1} ($\Gamma = 1.2$) the prolongation of the lifetime of a bubble with $R_b = 0.36$ mm is observed for the frequency range *ca.* 70–80 Hz while for the larger bubble with $R_b = 0.56$ mm the range is lower and equal to *ca.* 50–70 Hz. As one could expect, for a smaller bubble, more energy is required for suitable deformation (value of R_F) ensuring prolongation of

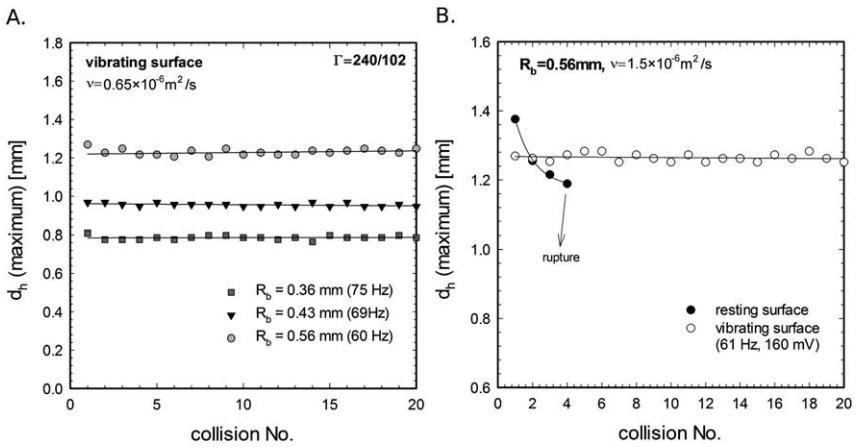

Fig. 9 Values of the bubbles' horizontal diameters at collision as a function of the collision number for vibrating and resting oil/air interfaces.

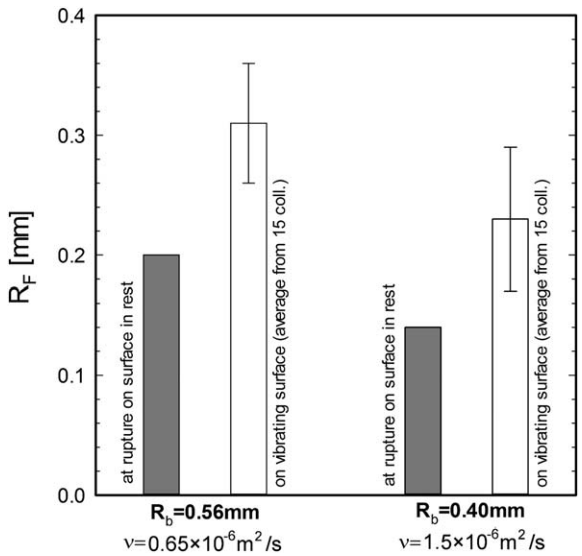

Fig. 10 Radius (dynamic) of the liquid film formed by the colliding bubble at the rupture collision with the oil surface at rest and during the collisions with the vibrating oil surface (average from 15 collisions).

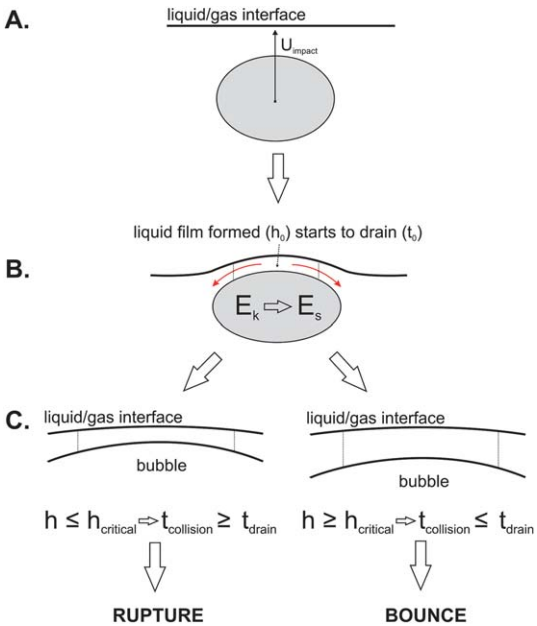

Fig. 11 Schematic presentation of the mechanism and parameters determining the outcome (bouncing or coalescence) of the bubble collision with the liquid/air interface.

bouncing. The dependence of the bouncing on the frequency is certainly related to the Rayleigh Eigen frequencies of the bubble.[14]

Fig. 11 presents schematically a mechanism and conditions needed for the bubble bouncing or rupture to occur at the liquid/air interface being at rest. The bubble collides with the liquid free surface with a defined impact velocity (kinetic energy E_k, associated with the bubble motion), equal to its terminal velocity when the interface is located far enough from the point of the bubble formation.[20,21] At the moment of collision, a liquid film between the bubble and the interface is formed. The liquid film is squeezed by the colliding bubble and its thickness starts to decrease as a result of the drainage process. Simultaneously, the kinetic energy associated with the bubble motion is transferred into surface energy (E_s) of the deformed bubble and liquid/air interfaces (interfacial area increases). The bubble pops or bounces according to the faster of both simultaneous processes.[2]

Conclusions

The mechanism of a bubble bouncing at the liquid/air interface has been analyzed. It was found that the drainage time of the liquid film formed by the bubble colliding with the liquid/air interface is a parameter of crucial importance for the bouncing to occur. As the drainage time depends on deformation (radius of the liquid film), the bubble is allowed to bounce when this drainage time is longer than the contact time with the interface. The drainage time increases when the bubble deformation increases. The tracking of the motion and of the deformation of the bubble allowed deducing a criterion for rebound on the oil/air and water/air interfaces at rest. These results are the basis for explaining the increase of the lifetime of an air bubble at a vibrated interface. Above a threshold acceleration of the vibrated interface, the transfer of energy to the bubble is

sufficient to deform it such as to be in the bouncing condition, *i.e.* a large deformation that results increases the drainage time, which avoids coalescence. Further experiments will be performed in order to establish the relation between the frequency of excitation, the acceleration threshold and the bubble shape parameters.

Acknowledgements

The work was supported by the COST P21 "Physics of Droplets" network (ESF). Financial support from the Ministry of Science and Higher Education (grant Nr 45/N-COST/2007/0 and Iuventus Plus 0490/H03/2010/70) is acknowledged with gratitude. S.D. thanks FNRS for financial support. J. P. Lecomte (Dow Corning Belgium) is thanked for providing silicone oil DC200.

References

1 R. D. Kirkpatrick and M. J. Lockett, *Chem. Eng. Sci.*, 1974, **29**, 2363.
2 A. K. Chester and G. Hofman, *Appl. Sci. Res.*, 1982, **38**, 353.
3 L. Doubliez, *Int. J. Multiphase Flow*, 1991, **17**(6), 783.
4 H.-K. Tsao and D. L. Koch, *Phys. Fluids*, 1994, **6**(8), 2591.
5 P. C. Duineveld, PhD thesis, Bouncing and Coalescence of Two bubbles in water, P. C. Duineveld, Enschede, 1994.
6 M. Krzan, K. Lunkenheimer and K. Malysa, *Langmuir*, 2003, **19**, 6586.
7 J. Zawala, M. Krasowska, T. Dabros and K. Malysa, *Can. J. Chem. Eng.*, 2008, **85**, 669.
8 T. Sanada, M. Watanabe and T. Fukano, *Chem. Eng. Sci.*, 2005, **60**, 5372.
9 F. Sunol and R. González-Cinca, *Colloids Surf., A*, 2010, **365**, 36.
10 J. Zawala and K. Malysa, *Langmuir*, 2011, **27**, 2250, DOI: 10.1021/la104324u (available online).
11 Y. Couder, E. Fort, C.-H. Gautier and A. Boudaoud, *Phys. Rev. Lett.*, 2005, **94**, 177801.
12 A. Eddi, E. Fort, F. Moissy and Y. Couder, *Phys. Rev. Lett.*, 2009, **102**, 240401.
13 E. Fort, A. Eddi, A. Boudaoud, J. Moukhtar and Y. Couder, *Proc. Natl. Acad. Sci. U. S. A.*, 2010, **107**, 17515.
14 T. Gilet, D. Terwagne, N. Vandewalle and S. Dorbolo, *Phys. Rev. Lett.*, 2008, **100**, 167802.
15 S. Dorbolo, D. Terwagne, N. Vandewalle and T. Gilet, *New J. Phys.*, 2008, **10**, 113021.
16 T. Tate, *Philos. Mag.*, 1864, **27**, 176.
17 A. W. Adamson, *Physical Chemistry of Surfaces*, John Wiley&Sons, Inc., 1990, p. 21.
18 A. Scheludko, *Adv. Colloid Interface Sci.*, 1967, **1**, 391.
19 N. Tufillaro, T. Abbott and J. Reilly, *An experimental approach to nonlinear dynamics and chaos*, New York, Addison-Wesley, 1992.
20 K. Malysa, M. Krasowska and M. Krzan, *Adv. Colloid Interface Sci.*, 2005, **114–115**, 205.
21 M. Krzan, J. Zawala and K. Malysa, *Colloids Surf., A*, 2007, **298**, 42.

